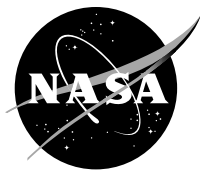


NASA/TM—2016-218943



# Advanced Face Gear Surface Durability Evaluations

*David G. Lewicki*

*U.S. Army Research Laboratory, Glenn Research Center, Cleveland, Ohio*

*Gregory F. Heath*

*The Boeing Company, Mesa, Arizona*

## **Notice for Copyrighted Information**

This manuscript is a joint work of employees of the National Aeronautics and Space Administration and employees of The Boeing Company under Agreement No. W911W6-06-2-0006 with the National Aeronautics and Space Administration. The United States Government may prepare derivative works, publish or reproduce this manuscript, and allow others to do so. Any publisher accepting this manuscript for publication acknowledges that the United States Government retains a nonexclusive, irrevocable, worldwide license to prepare derivative works, publish or reproduce the published form of this manuscript, or allow others to do so, for United States Government purposes.

## NASA STI Program . . . in Profile

Since its founding, NASA has been dedicated to the advancement of aeronautics and space science. The NASA Scientific and Technical Information (STI) Program plays a key part in helping NASA maintain this important role.

The NASA STI Program operates under the auspices of the Agency Chief Information Officer. It collects, organizes, provides for archiving, and disseminates NASA's STI. The NASA STI Program provides access to the NASA Technical Report Server—Registered (NTRS Reg) and NASA Technical Report Server—Public (NTRS) thus providing one of the largest collections of aeronautical and space science STI in the world. Results are published in both non-NASA channels and by NASA in the NASA STI Report Series, which includes the following report types:

- **TECHNICAL PUBLICATION.** Reports of completed research or a major significant phase of research that present the results of NASA programs and include extensive data or theoretical analysis. Includes compilations of significant scientific and technical data and information deemed to be of continuing reference value. NASA counter-part of peer-reviewed formal professional papers, but has less stringent limitations on manuscript length and extent of graphic presentations.
- **TECHNICAL MEMORANDUM.** Scientific and technical findings that are preliminary or of specialized interest, e.g., “quick-release” reports, working papers, and bibliographies that contain minimal annotation. Does not contain extensive analysis.
- **CONTRACTOR REPORT.** Scientific and technical findings by NASA-sponsored contractors and grantees.
- **CONFERENCE PUBLICATION.** Collected papers from scientific and technical conferences, symposia, seminars, or other meetings sponsored or co-sponsored by NASA.
- **SPECIAL PUBLICATION.** Scientific, technical, or historical information from NASA programs, projects, and missions, often concerned with subjects having substantial public interest.
- **TECHNICAL TRANSLATION.** English-language translations of foreign scientific and technical material pertinent to NASA's mission.

For more information about the NASA STI program, see the following:

- Access the NASA STI program home page at <http://www.sti.nasa.gov>
- E-mail your question to [help@sti.nasa.gov](mailto:help@sti.nasa.gov)
- Fax your question to the NASA STI Information Desk at 757-864-6500
- Telephone the NASA STI Information Desk at 757-864-9658
- Write to:  
NASA STI Program  
Mail Stop 148  
NASA Langley Research Center  
Hampton, VA 23681-2199



# Advanced Face Gear Surface Durability Evaluations

*David G. Lewicki*

*U.S. Army Research Laboratory, Glenn Research Center, Cleveland, Ohio*

*Gregory F. Heath*

*The Boeing Company, Mesa, Arizona*

## **Notice for Copyrighted Information**

This manuscript is a joint work of employees of the National Aeronautics and Space Administration and employees of The Boeing Company under Agreement No. W911W6-06-2-0006 with the National Aeronautics and Space Administration. The United States Government may prepare derivative works, publish or reproduce this manuscript, and allow others to do so. Any publisher accepting this manuscript for publication acknowledges that the United States Government retains a nonexclusive, irrevocable, worldwide license to prepare derivative works, publish or reproduce the published form of this manuscript, or allow others to do so, for United States Government purposes.

National Aeronautics and  
Space Administration

Glenn Research Center  
Cleveland, Ohio 44135

## Acknowledgments

This research was partially funded by the U.S. Army Aviation Applied Technology Directorate, Fort Eustis, Virginia 23604, under Agreement No. W911W6-06-2-0006.

*Level of Review:* This material has been technically reviewed by technical management.

Available from

NASA STI Program  
Mail Stop 148  
NASA Langley Research Center  
Hampton, VA 23681-2199

National Technical Information Service  
5285 Port Royal Road  
Springfield, VA 22161  
703-605-6000

This report is available in electronic form at <http://www.sti.nasa.gov/> and <http://ntrs.nasa.gov/>

# Advanced Face Gear Surface Durability Evaluations

David G. Lewicki\*  
National Aeronautics and Space Administration  
Glenn Research Center  
Cleveland, Ohio 44135

Gregory F. Heath  
The Boeing Company  
Mesa, Arizona 85215

## Abstract

The surface durability life of helical face gears and isotropic super-finished (ISF) face gears was investigated. Experimental fatigue tests were performed at the NASA Glenn Research Center. Endurance tests were performed on 10 sets of helical face gears in mesh with tapered involute helical pinions, and 10 sets of ISF-enhanced straight face gears in mesh with tapered involute spur pinions. The results were compared to previous tests on straight face gears. The life of the ISF configuration was slightly less than that of previous tests on straight face gears. The life of the ISF configuration was slightly greater than that of the helical configuration.

## Introduction

The Enhanced Rotorcraft Drive System (ERDS) program was a U.S. Army sponsored activity to develop critical performance and affordability enhancing drive system technologies for rotorcraft. The ERDS program goals were 40% increase in drive system transmitted horsepower-to-weight ratio, 15-dB reduction in drive system generated noise, 30% reduction in drive system production cost, 30% reduction in drive system operating and support costs, and 75% automatic detection of critical mechanical component failures. The ERDS program consisted of design, fabrication, and demonstration testing of critical drive system technologies required to achieve the program goals for the Army's current and future force fleet of rotorcraft. One such technology was advanced face gear development.

Previous studies showed that a split-torque, face-gear transmission gave a 40% decrease in weight potential compared to a conventional design for an advanced attack helicopter application (Ref. 1). Much work has been devoted in recent years in the analytical development of face gears, with emphasis on gear tooth geometry, tooth contact patterns, transmission error, gear tooth grinding methods, lubrication considerations, and torsional stability (Refs. 2 to 8). Recent experimental validation to determine surface durability life of face gears has been performed (Ref. 9). Here, face gears in mesh with tapered spur involute pinions were evaluated in support of U.S. Army fleet upgrades (Ref. 10). This design was further described in Reference 11 for use in the U.S. Army Apache Block III improved drive system.

To further enhance the power density of this unique split-torque face gear arrangement, helical face gear technology was developed as part of the ERDS program (Ref. 12). Analytical tools were developed to support ERDS helical face gear design and manufacture. Finite element non-linear contact analysis models were produced to determine stress distributions of gear teeth as the gears rolled through mesh under load. In addition, a second-generation face gear grinding machine was developed. This machine was aimed at production process enhancements of current straight face gears and involute pinions. Also, additional degrees of freedom were incorporated for the manufacturing of helical face gears meshing with helical tapered pinions. This machine was used to manufacture helical test gears for use in the NASA Glenn face-gear tests facility.

---

\*Retired.

In addition to helical face gears, enhanced straight face gears in mesh with tapered spur involute pinions were developed as part of the ERDS program. The gears were enhanced using the isotropic super-finishing (ISF) process (Ref. 13). Previous studies showed significant improvements in surface durability using the ISF process in certain applications (Refs. 14 and 15).

The objective of the current study is to determine the surface durability life of helical face gears and ISF face gears. Experimental fatigue tests were performed at the NASA Glenn Research Center. Endurance tests were performed on 10 sets of helical face gears in mesh with tapered involute helical pinions, and 10 sets of ISF-enhanced straight face gears in mesh with tapered involute spur pinions. The results are compared to previous tests on straight face gears.

## **Apparatus**

### **Test Facility**

The experiments reported in this report were tested in the NASA Glenn spiral-bevel-gear/face-gear test facility. An overview sketch of the facility is shown in Figure 1(a) and a schematic of the power loop is shown in Figure 1(b). The facility operates in a closed-loop arrangement. A pinion drives a face gear in the test (left) section. The face gear drives a set of facility helical gears, which in turn, drive a face gear and pinion in the slave (right) section. The pinions of the slave and test sections are connected by a cross shaft, thereby closing the loop. Torque is supplied in the loop by physically twisting and locking a torque in the pre-load coupling on the slave section shaft. Additional torque is applied through a thrust piston, which exerts an axial force on one of the facility helical gears. The thrust piston is pressurized with facility oil through a high pressure pump. The total desired level of torque is achieved by adjusting the oil supply pressure to the piston using a closed-loop control servovalve. A 100-hp DC drive motor, connected to the loop by V-belts and pulleys, controls the speed as well as provides power to overcome friction. The facility has the capability to operate at 750 hp and 20,000 rpm pinion speed. A torquemeter in the loop on the test side measures torque and speed. The facility is also equipped with thermocouples, oil flow meters, pressure transducers, accelerometers, counters, and shutdown instrumentation to allow 24-hour unattended operation.

The test gears and facility bearings and gears were lubricated and cooled by a pressurized oil system. The lubricating fluid used was a synthetic base helicopter transmission oil conforming to the DOD-L-85734 specification. The test pinions and face gears were lubricated by jets which radially directed oil into the roots of the teeth on both the into-mesh and out-of-mesh sides. The nominal oil supply pressure was 80 psi and the nominal flow rate was 1.0 gpm for each the test section and slave section. Oil inlet temperature was set at 100 °F. An external vacuum pump connected to the oil tank worked as a scavenge system to remove the oil from the test gearboxes and bearing cavities and direct it to the sump. Also, the oil system was equipped with an oil-debris monitor as well as a three-micron filter.

### **Test Gears**

Three different design configurations were tested in this study. As previously mentioned, a second-generation face gear grinding machine was developed to manufacture enhanced-straight and helical test gears. This machine was used to manufacture all test gears in this study. The first configuration was the baseline and was that identified as Mod3 in Reference 9 and used in previous endurance tests. Four sets of this design were tested. The second configuration was the same as the baseline but used the isotropic super-finishing (ISF) process as the final step. Ten sets of this design were tested. The third set was comprised of helical gears, primarily based on the baseline, but with a relatively small helix angle. Ten sets of this design were tested.

The design parameters for the pinions and face gears of the ISF test set are given in Table I. A photograph of this test set is shown in Figure 2(a). Other than surface finish, all parameters were the same as the baseline Mod3 design. The set was primarily designed to fail in surface pitting contact fatigue mode. The set had a reduction ratio of 3.842:1 and a diametral pitch of 10.6 teeth/in., roughly similar to the current AH-64 helicopter replacement design. The face width of the face gears was 0.6 in. The face width of the spur pinions was 0.8 in., significantly greater than the face gear to allow for axial adjustment required for backlash adjustment and optimization of tooth contact. The shaft angle was 90° to accommodate the test facility. The pinions were slightly tapered with a half cone angle of 4.2°. This was similar to the current AH-64 replacement design and allows the independent setting of backlash for the multiple pinions and idlers in the split-torque transmission application (Ref. 16). The surface finish specification of the ISF design was 3 to 5  $\mu\text{in. } R_{rms}$ .

The design parameters for the pinions and face gears of the helical test set are also given in Table I. A photograph of this test set is shown in Figure 2(b). The helical set design was similar to the baseline/ISF design with the same numbers of teeth, pressure angle, and shaft angle. The helix angle was 10°. This angle approached the maximum allowed on the current manufacturing machine. The face widths of the helical set were less than the baseline/ISF (0.5 in. for the face gear, 0.7 in. for the pinion) and the diametral pitch was slightly greater (10.7 teeth/in.). This was chosen to achieve the approximate same compressive tooth stress per unit load for all design configurations.

All test gears were made from carburized and ground vacuum induction melting-vacuum arc remelting (VIM-VAR) Pyrowear 53 steel per AMS 6308 using standard aerospace practices. At 6000 lb-in. face gear torque, the calculated AGMA contact stress index was 250 ksi using approximate spur gear calculations per (Ref. 17).

## Test Gear Installation Procedure

Previous studies showed that proper pinion and face gear installation is a criteria for successful operation. This was true for both straight spur involute pinions in mesh with a face gear (Ref. 18) and tapered spur involute pinions in mesh with a face gear (Ref. 9). In the current study, the effect of pinion and face gear installation for helical gears was investigated. Figure 3 shows the pinion and face gear position adjustments studied. These adjustments were achieved by moving the axial position of either the face gear or pinion by changing shim sizes behind the face gear or behind the pinion housing. Increasing the shim size behind the face gear moved the gear further into mesh. Decreasing the shim size behind the pinion housing moved the pinion further into mesh due to the tapered profile of the pinion tooth.

Backlash measurements were made by locking the pinion and measuring the movement of the face gear using a dial indicator while manually rocking the face gear back and forth. No load contact pattern measurements were made by applying marking compound to the pinions and face gears and manual turning the gears through mesh under no applied rig torque but slight hand resistance. Figure 4 shows the effect of face gear adjustments on no-load contact pattern and backlash while keeping a constant pinion position. It is clear that the face gear adjustment had a significant effect on both pattern and backlash. Moving the face gear into mesh by increasing the shim size decreased backlash and moved the contact pattern from toe to heel. On the other hand, moving the face gear out of mesh by decreasing the shim size increased backlash and moved the contact pattern from heel to toe. Figure 5 shows the effect of pinion adjustments on contact pattern and backlash while keeping a constant face gear position. Moving the pinion into mesh by decreasing the shim size decreased backlash, but had a relatively small effect on the face gear tooth contact pattern for the range of adjustments used. Moving the pinion out of mesh by increasing the shim size increased backlash, and also had a relatively small effect on the face gear tooth contact pattern. As expected, the contact pattern on the pinion tooth moved from heel to toe as the pinion was moved out of mesh (backlash increased), and from toe to heel as the pinion was moved into mesh (backlash decreased). However, since the pinion tooth width was wider than the face gear tooth width, the patterns still remained on the tooth. Thus, adjusting the pinion position was an effective way of adjusting backlash without severely affecting the contact pattern.

From the studies, the effect of pinion and gear installation of the helical test sets was very similar to that of the tapered spur involute pinions and face gear sets of Reference 9. Figure 6 compares the backlash as a function of gear shim and pinion shim for the two configurations. From Figure 6(a), the slopes of the backlash versus gear shim curve fits were nearly identical for the two configurations with a slight offset. From Figure 6(b), the backlash versus pinion shim curve fits were nearly the same. Thus, the same trend occurred for both the helical and spur sets and the same installation procedure was used for both.

The installation procedure from Reference 9 was used for all the gears tested and was defined as follows. First, the test-side pinion and face gear were installed in the facility (with no cross shaft connected to the pinion). Backlash measurements and no-load contact pattern checks were taken for the mesh. A contact pattern biased slightly toward the heel on the face gear and a backlash of 0.006 to 0.010-in. was required. The slight bias of pattern was required since the pattern shifted slightly toward the toe when full load was applied. The face gear shim was first adjusted to achieve the proper contact pattern, and then the pinion shim was adjusted to achieve the proper backlash. This process was then repeated for the slave-side pinion/face-gear mesh. Figure 7 shows an acceptable no-load contact pattern for the helical gear set and Figure 8 shows an acceptable no-load contact pattern for the ISF gear set. After proper shimming was achieved, the cross shaft was installed. Marking compound was then re-applied to all the pinions and gears and a loaded static roll test was performed. This was done by applying a moderate torque in the loop (through the load piston), manually rotating the complete assembly, and photographing the resulting contact patterns. The objective of this procedure was to ensure that proper backlash and proper shimming was used, edge loading was prevented, and the contact pattern on the face-gear tooth was evenly spread under load.

Before beginning the endurance tests, a speed sweep survey was conducted. Two sets of helical test gears were installed per above and run at from 1500 to 3900 rpm gear speed in 100 rpm increments. Vibration data were collected from accelerometers mounted on the left and right side pinion housings. The objective was to identify resonant operating conditions to avoid during test. Figure 9 shows waterfall spectra of the two accelerometers. The majority of the vibration was at the fundamental, second, and third gear mesh frequencies. Resonant conditions were evident from approximately 2400 to 3000 rpm gear speed. These were increases of housing vibrations excited by gear mesh frequencies. Also, higher frequency vibration was observed at speeds greater than 3000 rpm. From these results, 2200 rpm gear speed was chosen as the operating speed for the endurance tests.

## **Test Procedure**

The test procedure to evaluate the fatigue life of face gears was as follows. First, the selected test gears were installed with the proper shims as described above. Backlash measurements as well as unloaded and loaded contact patterns were documented. After acceptable patterns and backlash, the gears were then run through a break-in procedure described in Table II. This was a short 70-min run consisting of a gradual increase in speed and torque. The applied torque was obtained using only the load piston. After completion of the break-in run, the gears were inspected. The pre-load coupling was then adjusted to produce a face-gear torque somewhere between 3000 to 5000 lb-in. The gears were then run at 2200 rpm gear speed and 7200 lb-in. gear torque (torque adjusted using load piston). Facility parameters such as speed, torque, oil pressure, oil flow, housing vibration, and a variety of component temperatures were collected. In addition, high-frequency vibration monitoring with gear fault detection software and oil-debris monitoring (Ref. 19) were collected. During the tests, the gears were inspected at routine intervals (5 to 10 million face gear cycles). The gears were run until surface pitting occurred or a suspension was defined. Once completed, the gears were removed from the facility, cleaned, and photographed for documentation purposes.



## **Results and Discussion**

### **Pre-endurance Test Screening**

Four sets of the baseline configuration were tested at the start of the project. This gear design was that identified as Mod3 in Reference 9 but fabricated on the second-generation face gear grinding machine. The purpose of these tests was to validate the manufacturing capabilities of the second grinding machine on a proven design configuration. The sets were run at 2300 rpm gear speed and 7200 lb-in. gear torque. Each set was run for 38.4 M pinion cycles. After test, the gears were inspected. None exhibited surface pitting fatigue and all encountered wear similar to that experienced in Reference 9, thus giving confidence in the new grinding machine. The results are summarized in Table III.

### **Helical Test Gear Results**

Ten sets of helical gears were tested. The sets were run at 2200 rpm gear speed and 7200 lb-in. gear torque. Table IV summarizes the test results. Eight of the ten sets tested failed in surface pitting contact fatigue. The failures were either progressive or spalling macropitting contact fatigue as described in Reference 20. Per the project test plan, failure was defined as macropitting of at least 0.10-in. continuous length along the contact area on any tooth of one of the tested pinions or gears. Of the failures, 6 of the 10 pinions failed in macropitting and 3 of the 10 face gears failed in macropitting. In some cases, pinion tooth fracture occurred where the fracture originated from pits on the tooth contacting surface. The contact fatigue failure times ranged from 26.5 to 80.3 M pinion cycles (Table IV). These times were either run times at inspection or adjusted run times based on a clear indication of failure from the gear fault detection vibration instrumentation and software. All test gears exhibited moderate adhesion wear and/or micropitting contact fatigue (as described in Ref. 20) due to the relatively high contact stress operating conditions.

Figure 10 shows photographs of typical contact fatigue failures of helical test gear sets. Shown are examples of pinion progressive and spalling macropitting contact fatigue as well as an example of face gear spalling macropitting contact fatigue. Figure 11 shows a Weibull plot of the results from the helical test gear sets. The method of Johnson (Ref. 21) was used to derive the plot. The procedure plots the medium rank of the data point as a function of number of cycles. The medium rank is also adjusted when suspensions occur. The data is plotted on special Weibull logarithmic axes. The solid line is the linear regression fit of the data. Also included in the plot are 90% confidence bands as shown by the dotted lines. It should be noted that even though 8 failures occurred, the results of not statistically strong as indicated by the relatively large scatter in life for the 90% confidence bands, especially at lower percentages of failure.

### **Isotropic Super-Finish (ISF) Test Gear Results**

Ten sets of ISF gears were tested. The sets were run at 2200 rpm gear speed and 7200 lb-in. gear torque. Table V summarizes the test results. Nine of the ten sets tested failed in surface pitting contact fatigue. The failures were either progressive or spalling macropitting contact fatigue. Of the failures, 6 of the 10 pinions failed in macropitting and 4 of the 10 face gears failed in macropitting. No pinion tooth fracture occurred for any of the sets. The contact fatigue failure times ranged from 38.4 to 156.9 M pinion cycles (Table V). Most test gears exhibited micropitting contact fatigue at the tips or roots of the contact zone, but significantly less moderate adhesion wear occurred as compared to the helical sets.

Figure 12 shows photographs of typical contact fatigue failures of ISF test gear sets. Shown are examples of pinion progressive and spalling macropitting contact fatigue as well as an example of face gear progressive macropitting contact fatigue. Figure 13 shows a Weibull plot of the results from the helical test gear sets.

## Comparison of Results

Figure 14 compares the life results of the helical test gear sets, ISF test gear sets, and RDS21 test gear sets as shown in a single Weibull plot. The data for the helical sets is that from Figure 11. The data for the ISF sets is that from Figure 13. The data for the RDS21 sets is that from (Ref. 9) run at 7200 lb-in. gear torque. The RDS21 set is the baseline design identified as Mod3 in Reference 9. Plotted in the figure are the median ranks versus life data points and linear curve fits of each design. As seen in the figure, the life of the RDS21 sets was slightly greater than that of the ISF sets, and the life of the ISF sets was slightly greater than that of the helical sets.

The lives are further quantized in Table VI. In the table, the  $L_1$ ,  $L_{10}$ ,  $L_{50}$ , and  $L_{mean}$  are the lives for 1% probability of failure, 10% probability of failure, 50% probability of failure, and mean lives, respectively. These are given for the median rank curve fit as well as lower and upper 90% confidence intervals. Also given are the Weibull slopes of the median rank linear curve fit, which measure scatter in the data (larger slopes indicate greater scatter). The  $L_{10}$  life of the RDS21 sets is 1.52x greater than that of the ISF sets, and the  $L_{10}$  life of the RDS21 sets is 2.03x greater than that of the helical sets. The  $L_{mean}$  life of the RDS21 sets is 1.40x greater than that of the ISF sets, and the  $L_{mean}$  life of the RDS21 sets is 2.35x greater than that of the helical sets. Even though 10 sets each of the helical and ISF configurations were tested and 17 failures were produced, more data was needed to produce statistically significant results. This can be seen by the larger scatter in lives at the 1 and 10% probabilities of failure levels. These levels are more important in analyzing gear data for rotorcraft applications since no gear failures can be tolerated in practice.

The statistical significance is also evident in Table VII where the significance of the resulting lives of the helical and ISF sets are compared to RDS21 lives. This table was created using the methods of Johnson (Ref. 21) in which the confidence that the lives of a tested population are greater (or less) than those of another tested population is explored. This confidence is based on the sample sizes (number of failures for both populations) and life ratios of the populations, either at the  $L_{10}$  life or  $L_{mean}$  life level. From Table VII, the confidence of the  $L_{10}$  life of the helical sets relative to the RDS21 sets is 78%. This means that 78 times out of 100, the  $L_{10}$  population life of the helical sets is less than that of the RDS21 sets. The confidence of the  $L_{10}$  life of the ISF sets relative to the RDS21 sets is only 64%. Confidence numbers in the 70 to 80% range are rather marginal in significance. Numbers in the 50 to 60% range indicate no significant difference. The only conclusion that can be drawn with high confidence is that the mean life of the helical sets is statistically less than the mean life of the RDS21 sets (confidence >99%).

The results of the endurance tests were surprising. The helical gears sets were designed for approximately the same contact stress per unit load as the RDS21 sets using AGMA calculations for spur and helical gears (Ref. 17). The resulting lives of the helical sets, however, were lower than those of the RDS21 sets. The lives of the ISF sets were expected to be greater than those for the RDS21 sets. Based on the lambda ratio (defined as calculated film thickness using spur gear approximations divided by surface roughness) and results from previous gear life tests (Ref. 22), the lives of the ISF sets were expected to be three times that of the RDS21 sets. However, the ISF lives from the tests were slightly less but not significantly different than the RDS21 sets. The test gears of the current study were manufactured from a different lot of material than the RDS21 gears, which may be one explanation of the surprising results. A limited number of dimension and hardness inspections were performed on the test gear batch. However, no abnormalities were discovered. Also, the grinding process for helical face gears was somewhat further refined during manufacture and pattern development of full size helical face gears, done subsequent to the manufacture of the NASA helical face gears covered in this report. Another possibility in the discrepancy of results is that the approximate calculations for stress and film thickness that used spur and helical gears may not be truly reflective for face gear geometry. A more refined stress analysis methodology has been developed and applied by Boeing for straight tooth face gears since the above tests, though not for helical face gears. Additional investigation is required.

## Conclusions

The surface durability life of helical face gears and ISF face gears was investigated. Experimental fatigue tests were performed at the NASA Glenn Research Center. Endurance tests were performed on 10 sets of helical face gears in mesh with tapered involute helical pinions, and 10 sets of ISF-enhanced straight face gears in mesh with tapered involute spur pinions. The results were compared to previous tests on straight face gears. The following results were obtained:

1. The  $L_{10}$  life of the RDS21 configuration was 1.52x greater than that of the ISF configuration. The  $L_{mean}$  life of the RDS21 configuration was 1.40x greater than that of the ISF.
2. The  $L_{10}$  life of the RDS21 configuration was 2.03x greater than that of the helical configuration. The  $L_{mean}$  life of the RDS21 configuration was 2.35x greater than that of the helical.
3. Nine out of 10 gear sets failed in surface pitting fatigue for the ISF configuration, 8 out of 10 for the helical configuration, and 7 out of 12 for the RDS21 configuration. More data, however, was needed for statistically significant results.
4. The effect of gear installation of the helical test sets was very similar to that for the tapered spur involute test sets, giving similar backlash and contact pattern results.

## References

1. Heath, G.F., and Bossler, R.B., "Advanced Rotorcraft Transmission (ART) Program - Final Report," NASA Contractor Report CR-191057, Army Research Laboratory Contractor Report ARL-CR-14, McDonnell Douglas Helicopter Company, Contract NAS3-25454, Jan. 1993.
2. Litvin, F.L., Zhang, Y., Wang, J.-C., Bossler, R.B., and Chen, Y.-J.D., "Design and Geometry of Face-Gear Drives," ASME Journal of Mechanical Design, Vol. 114, No. 4, Dec. 1992, pp. 642-647.
3. Litvin, F.L., Wang, J.-C., Bossler, R.B., Chen, Y.-J.D., Heath, G.F., and Lewicki, D.G., "Application of Face-Gear Drives in Helicopter Transmission," ASME Journal of Mechanical Design, Vol. 116, No. 3, Sep. 1994, pp. 672-676.
4. Weck, M., Hurasky-Schonwerth, O., and Yakaria, H., "Manufacturing Simulation for Generation Grinding of Face Gears," Proceedings of the International Conference on Gears, Vol. I, Munich, Germany, Mar. 13-15, 2002, pp. 379-394.
5. Litvin, F.L., Fuentes, A., Zanzi, C., and Pontiggia, M., "Face Gear Drive with Spur Involute Pinion: Geometry, Generation by a Worm, Stress Analysis; Final Report," NASA Contractor Report CR-2002-211362, Army Research Laboratory Contractor Report ARL-CR-491, The University of Illinois at Chicago, Contract NAG3-2450, Feb. 2002.
6. Guingand, M., Vaujany, J.-P., and Jacquin, C.-Y., "Quasi-static analysis of a face gear under torque," Computer Methods in Applied Mechanics and Engineering, Vol. 194, No. 39-41, Oct. 2005, pp. 4301-4318.
7. Saribay, Z., Bill, R., Rao, S., and Smith, E., "Elastohydrodynamic Lubrication Analysis of Meshing Conjugate Face-Gear Pairs for Pericyclic Transmissions," Proceedings of the American Helicopter Society 66th Annual Forum, Phoenix, AZ, May 11-13, 2010.
8. Peng, M., and DeSmidt, H.A., "Torsional Stability of a Face-Gear Drive System," Proceedings of American Helicopter Society 68th Annual Forum, Ft. Worth, TX, May 1-3, 2012.
9. Lewicki, D.G., Heath, G.F., Filler, R.R., Slaughter, S.C., and Fetty, J., "Face-Gear Surface Durability Investigations," Journal of the American Helicopter Society, Vol. 53, No. 3, Jul. 2008, pp. 282-289.
10. Heath, G.F., Slaughter, S.C., Morris, M.T., Fetty, J., Lewicki, D.G., and Fisher, D.J., "Face Gear Development under the Rotorcraft Drive System for the 21st Century Program," Proceedings of the 65th American Helicopter Society International Forum, Grapevine, TX, May 27-29, 2009.
11. Gilbert, R., Craig, G., Filler, R., Hamilton, W., Hawkins, J., Higman, J., and Green, W., "3400 HP Apache Block III Improved Drive System," Proceedings of American Helicopter Society 64th Annual Forum, Montreal, Canada, Apr. 29 – May 1, 2008.

12. Heath, G., Slaughter, S., Fisher, D., Lewicki, D., and Fetty, J., "Helical Face Gear Development Under the ERDS Program," Proceedings of American Helicopter Society 67th Annual Forum, Virginia Beach, VA, May 3-5, 2011.
13. Michaud, M., Sroka, G., and Winkelmann, L., "Chemically Accelerated Vibratory Finishing for the Elimination of Wear and Pitting of Alloy Steel Gears," Proceedings of the Fall Technical Meeting of the American Gear Manufacturers Association 2001, Paper No. 01FTM7, Detroit, MI, Oct. 3-5, 2001.
14. Krantz, T.L., Alanou, M.P., Evans, H.P., and Snidle, R.W., "Surface Fatigue Lives of Case-Carburized Gears with an Improved Surface Finish," Proceedings of the DETC2000 8th International Power Transmission and Gearing Conference, Baltimore, MD, Sep. 10-13, 2000.
15. Sroka, G., and Winkelmann, L., "Superfinishing Gears: The State of the Art," Gear Technology, Vol. 20, No. 6, 2003, pp. 28-33.
16. Heath, G.F., Filler, R.R., and Tan, J., "Development of Face Gear Technology for Industrial and Aerospace Power Transmission," NASA Contractor Report CR-2002-211320, Army Research Laboratory Contractor Report ARL-CR-0485, The Boeing Company, Cooperative Agreement NCC3-356, May 2002.
17. ANSI/AGMA 2001-C95, "Fundamental Rating Factors and Calculation Methods for Involute Spur and Helical Gear Teeth," The American Gear Manufacturers Association, 2001.
18. Lewicki, D.G., Handschuh, R.F., Heath, G.F., and Sheth, V., "Evaluation of Carburized and Ground Face Gears," Journal of the American Helicopter Society, Vol. 45, No. 2, Apr. 2000, pp. 118-124.
19. Dempsey, P.J., "Data Fusion Tool for Spiral Bevel Gear Condition Indicator Data," Proceedings of the Society for Machinery Failure Prevention Technology for the Society's 68th Conference, May 20-22, 2014.
20. ANSI/AGMA 1010-E95, "Appearance of Gear Teeth - Terminology of Wear and Failure," The American Gear Manufacturers Association, 2007.
21. Johnson, L., The Statistical Treatment of Fatigue Experiments, Elsevier, New York, 1964.
22. Krantz, T.L., "On the Correlation of Specific Film Thickness and Gear Pitting Life," presented at the 2014 American Gear Manufacturers Association Fall Technical Meeting, Arlington, VA, Oct. 12-14, 2014.

TABLE I.—TEST GEAR DESIGN DATA

	ISF set	Helical set
AGMA quality	12	12
Number of teeth; pinion, gear	19, 73	19, 73
Diametral pitch, (teeth/in)	10.6	10.7
Pressure angle (deg)	27.5	27.5
Shaft angle (deg)	90	90
Helix angle (deg)	0	10
Face width (in); pinion, gear	0.8, 0.6	0.7, 0.5
Hardness (R <sub>c</sub> ); case, core	62, 38	62, 38
Surface finish, R <sub>rms</sub> (μin)	3-5	16
Material	X53 steel	X53 steel

TABLE II.—BREAK-IN RUN CONDITIONS

Step	Time, min	Face gear	
		Speed, rpm	Torque, lb-in.
1	10	700	335
2	10	1200	335
3	10	1800	835
4	10	2200	1670
5	10	2200	2505
6	10	2200	3340
7	10	2200	*

\*Highest torque achievable with load piston (ranged from 4000 to 6000 lb-in.).

TABLE III.—PRE-ENDURANCE TEST SCREENING STUDIES, BASELINE TEST GEAR SETS

Set no.	Installation side	Pinion S/N	Face gear S/N	M cycles (pinion)	Result
1	Left	ERDS0064	ERDS0004	38.4	Suspension
2	Right	ERDS0061	ERDS0002	38.4	Suspension
3	Right	ERDS0065	ERDS0003	38.4	Suspension
4	Left	ERDS0067	ERDS0005	38.4	Suspension

TABLE IV.—ENDURANCE TEST RESULTS, HELICAL TEST GEAR SETS

Set no.	Installation side	Pinion S/N	Face gear S/N	M cycles (pinion)	Result
5	Right	ERDS0078	ERDS0021	99.4	Suspension
6	Left	ERDS0082	ERDS0018	198.3	Suspension
7	Right	ERDS0083	ERDS0020	29.6	Failure
8	Right	ERDS0080	ERDS0019	67.2	Failure
9	Right	ERDS0085	ERDS0025	80.3	Failure
10	Left	ERDS0089	ERDS0023	28.7	Failure
11	Left	ERDS0090	ERDS0026	27.8	Failure
12	Left	ERDS0084	ERDS0024	26.5	Failure
13	Right	ERDS0086	ERDS0022	43.1	Failure
18	Left	ERDS0088	ERDS0027	32.3	Failure

TABLE V.—ENDURANCE TEST RESULTS, ISF TEST GEAR SETS

Set no.	Installation side	Pinion S/N	Face gear S/N	M cycles (pinion)	Result
14	Right	ERDS0071	ERDS0006	57.6	Failure
15	Left	ERDS0076	ERDS0013	96.1	Failure
16	Right	ERDS0073	ERDS0014	95.0	Suspension
17	Left	ERDS0068	ERDS0008	18.1	Failure
19	Left	ERDS0074	ERDS0016	118.5	Failure
20	Right	ERDS0069	ERDS0017	156.9	Failure
21	Left	ERDS0077	ERDS0015	75.9	Failure
22	Right	ERDS0072	ERDS0007	111.7	Failure
23	Left	ERDS0075	ERDS0011	74.3	Failure
24	Left	ERDS0070	ERDS0012	38.4	Failure

TABLE VI.—SUMMARY OF ENDURANCE TEST FATIGUE LIVES USING WEIBULL ANALYSIS

			Helical sets	ISF sets	RDS21 sets (Ref. 9)
Gear set life, M Cycles (pinion)	$L_1$	Lower 90% confidence limit	---	---	---
		Median rank curve fit	5.1	5.5	9.0
		Upper 90% confidence limit	28.2	39.6	53.8
	$L_{10}$	Lower 90% confidence limit	5.2	6.0	8.2
		Median rank curve fit	18.1	24.2	36.8
		Upper 90% confidence limit	37.6	55.0	87.0
	$L_{50}$	Lower 90% confidence limit	30.2	45.9	62.7
		Median rank curve fit	49.9	79.8	114.0
		Upper 90% confidence limit	73.6	123.5	180.8
	$L_{mean}$	Lower 90% confidence limit	33.6	53.9	72.4
		Median rank curve fit	53.9	90.4	126.9
		Upper 90% confidence limit	78.7	137.4	197.6
Weibull slope			1.86	1.58	1.67
Failure index			8 out of 10	9 out of 10	7 out of 12

TABLE VII.—SIGNIFICANCE OF FATIGUE LIVES RELATIVE TO RDS21 TEST GEAR SETS

	Helical sets	ISF sets
$L_{10}$	78%	64%
$L_{mean}$	>99%	87%

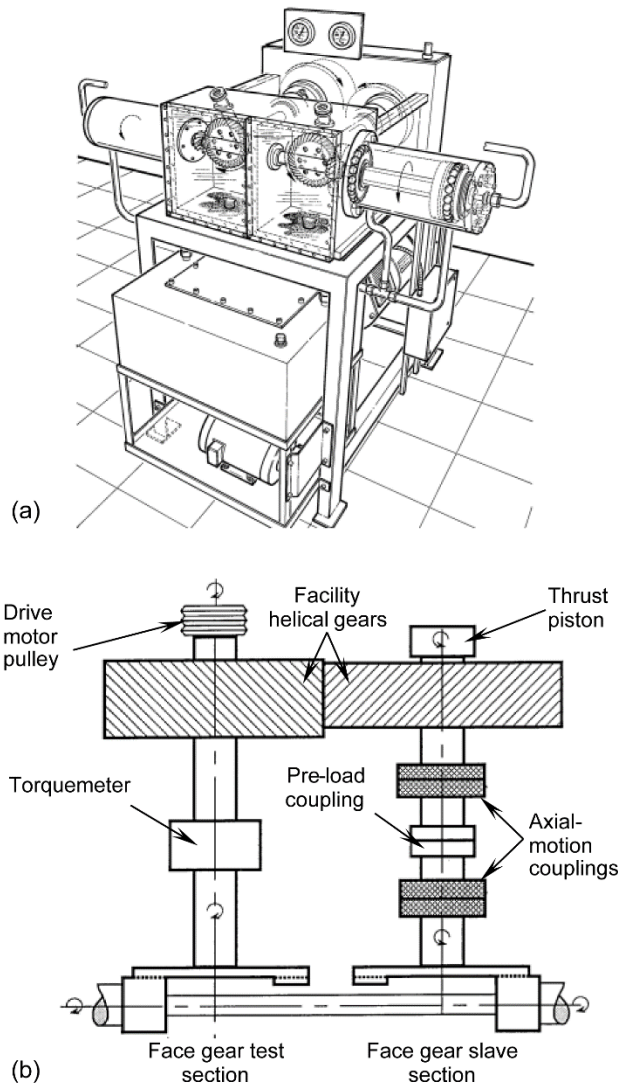


Figure 1.—NASA Glenn spiral-bevel-gear, face-gear test facility. (a) Overview of facility. (b) Schematic view.

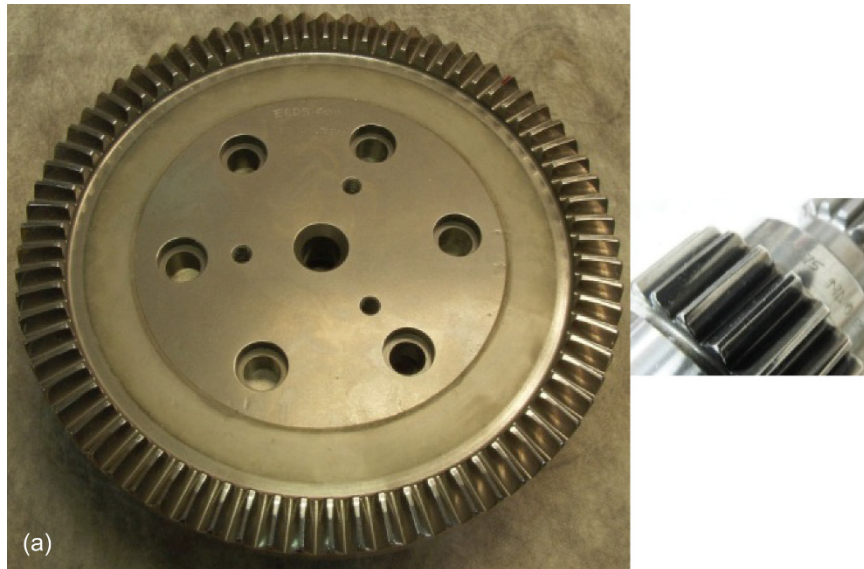


Figure 2.—Test gears. (a) Isotropic super-finished (ISF) test gears.  
(b) Helical test gears.



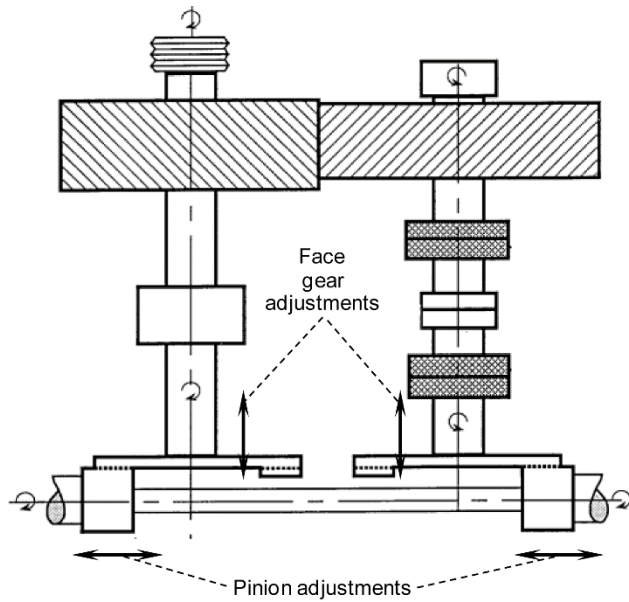


Figure 3.—Pinion and face gear position adjustments.

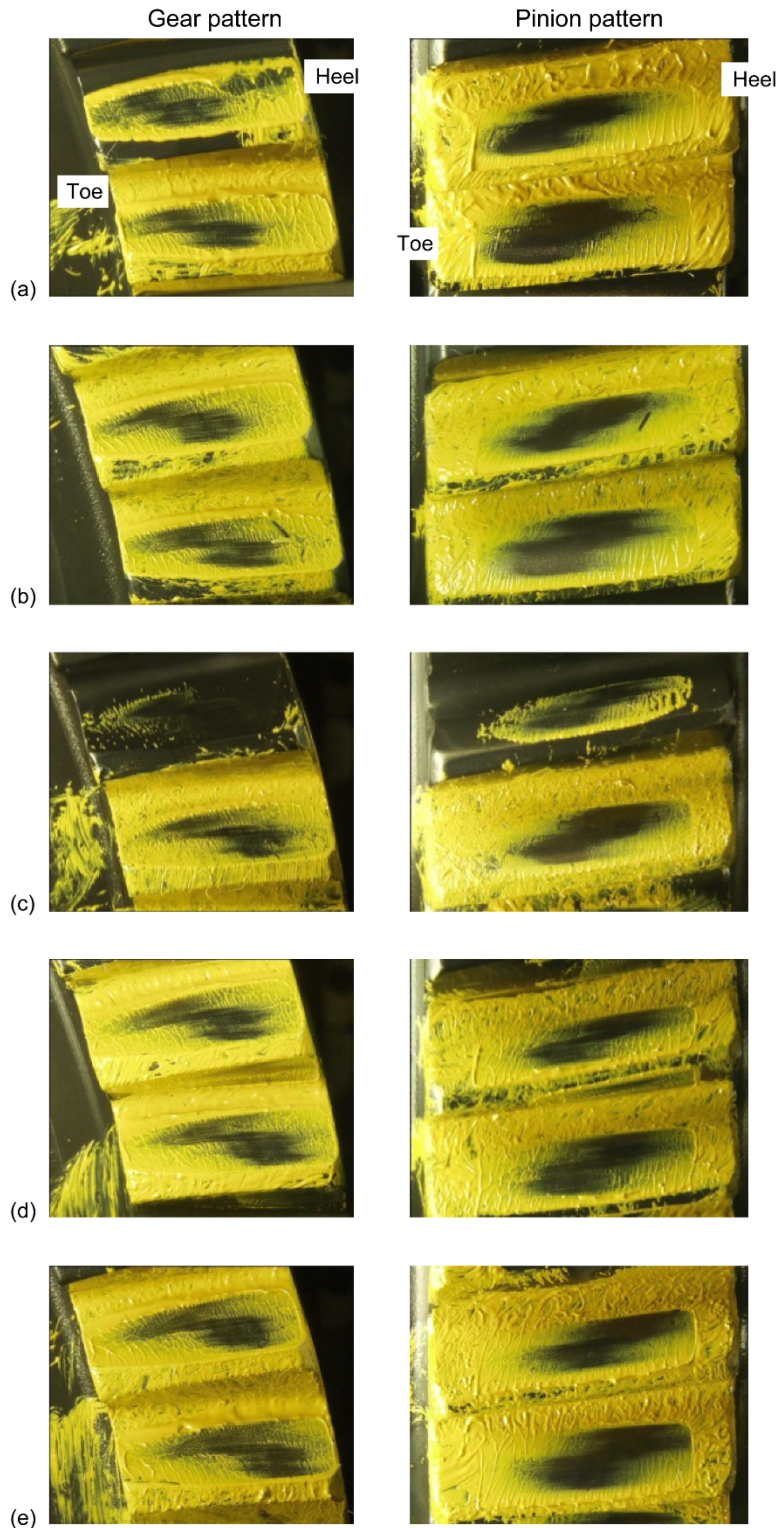


Figure 4.—Effect of gear shim on measured no-load contact pattern for helical test gear set. Pinion shim = 0.410 in.  
 (a) Gear shim = 0.094 in., backlash = 0.0162 in. (b) Gear shim = 0.096 in., backlash = 0.0147 in. (c) Gear shim = 0.098 in., backlash = 0.0092 in. (d) Gear shim = 0.100 in., backlash = 0.0075 in. (e) Gear shim = 0.102 in., backlash = 0.0027 in.

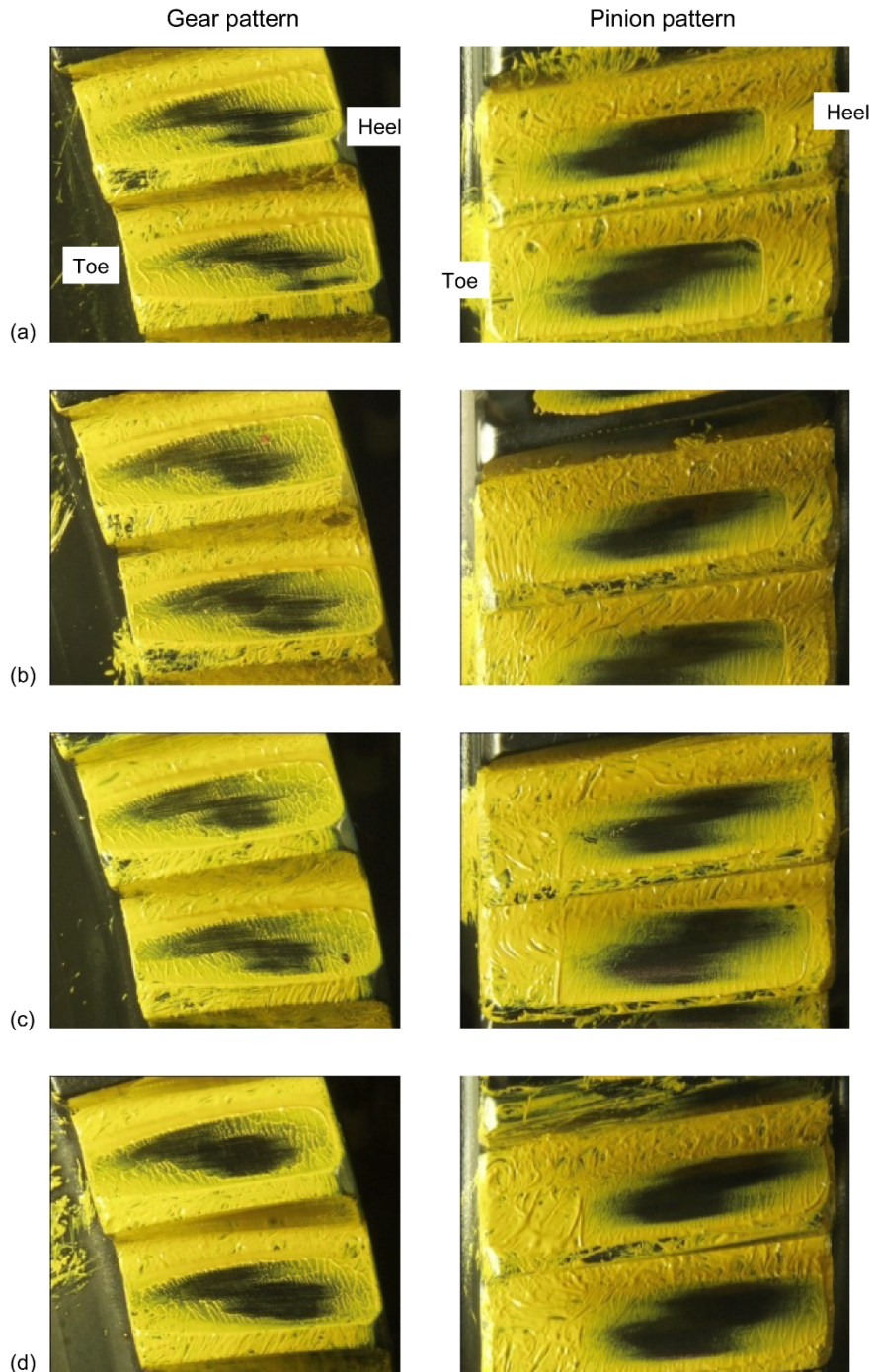


Figure 5.—Effect of pinion shim on measured no-load contact pattern for helical test gear set. Gear shim = 0.098 in. (a) Pinion shim = 0.460 in., backlash = 0.0148 in. (b) Pinion shim = 0.410 in., backlash = 0.0107 in. (c) Pinion shim = 0.360 in., backlash = 0.0052 in. (d) Pinion shim = 0.320 in., backlash = 0.0000 in.

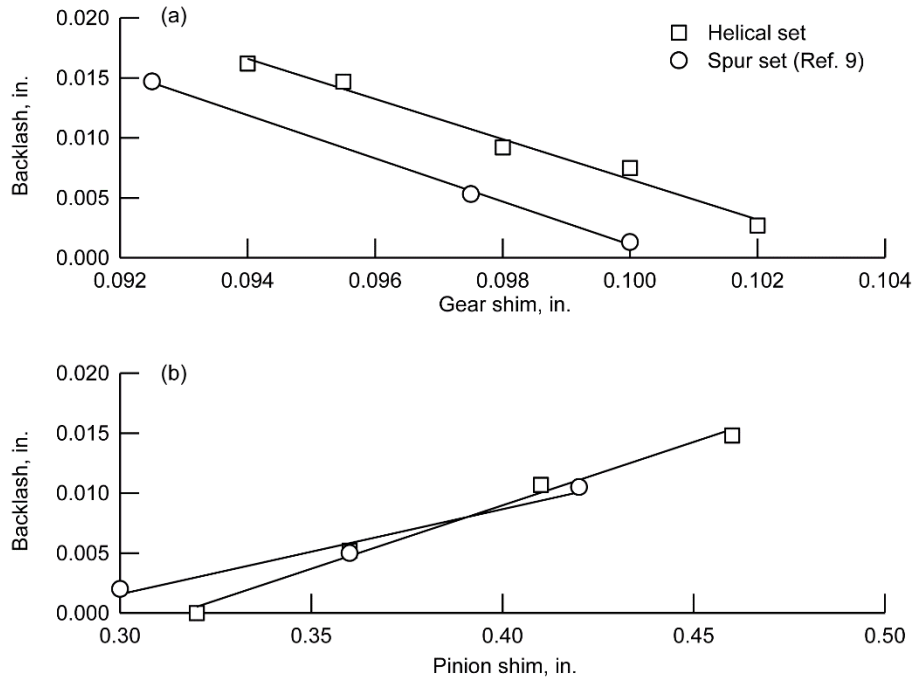


Figure 6.—Effect of shimming on measured backlash. (a) Gear shim effect.  
 (b) Pinion shim effect.

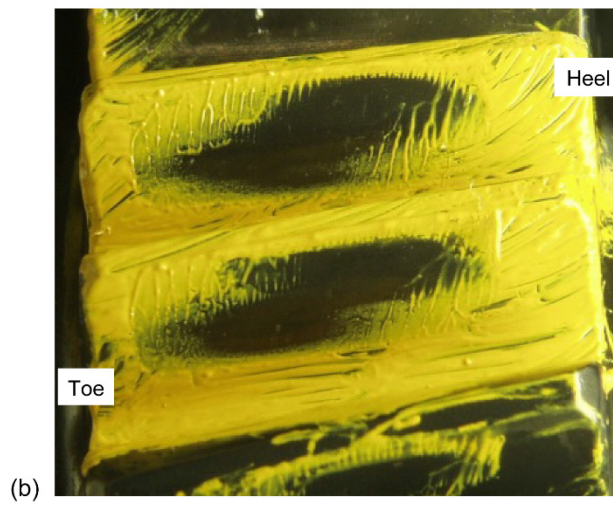
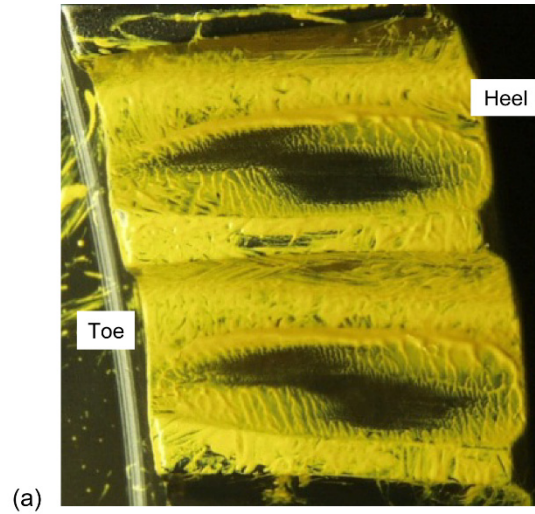
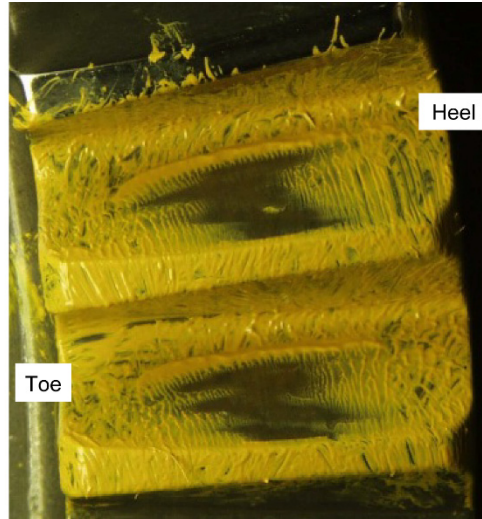
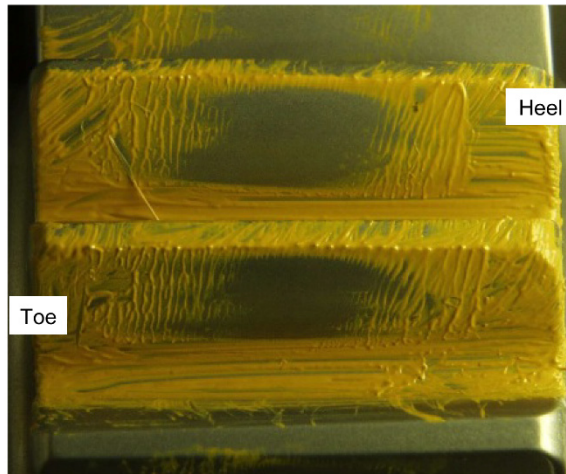


Figure 7.—Typical no-load contact pattern for helical test gear set. (a) Gear pattern. (b) Pinion pattern.



(a)



(b)

Figure 8.—Typical no-load contact pattern for ISF test gear set. (a) Gear pattern. (b) Pinion pattern.

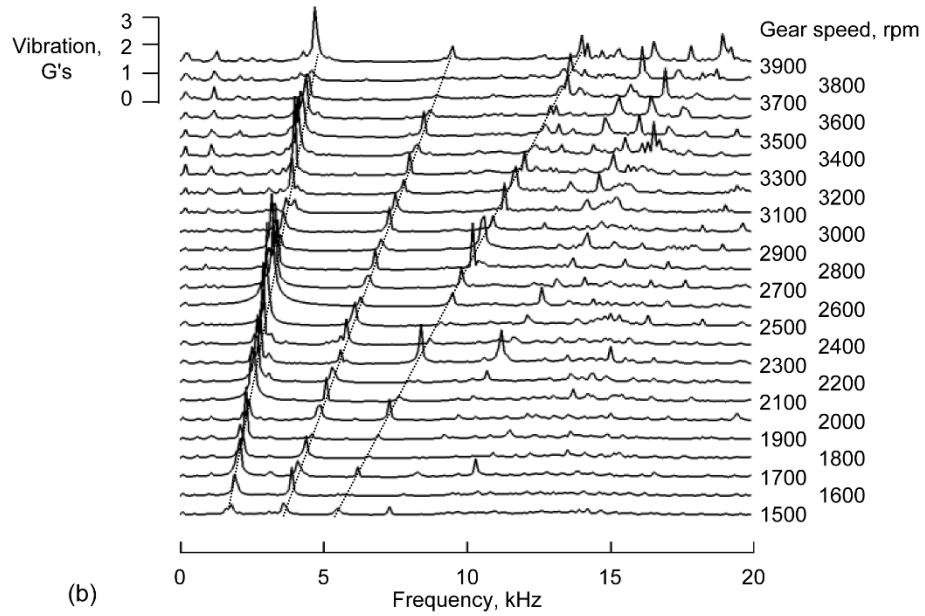
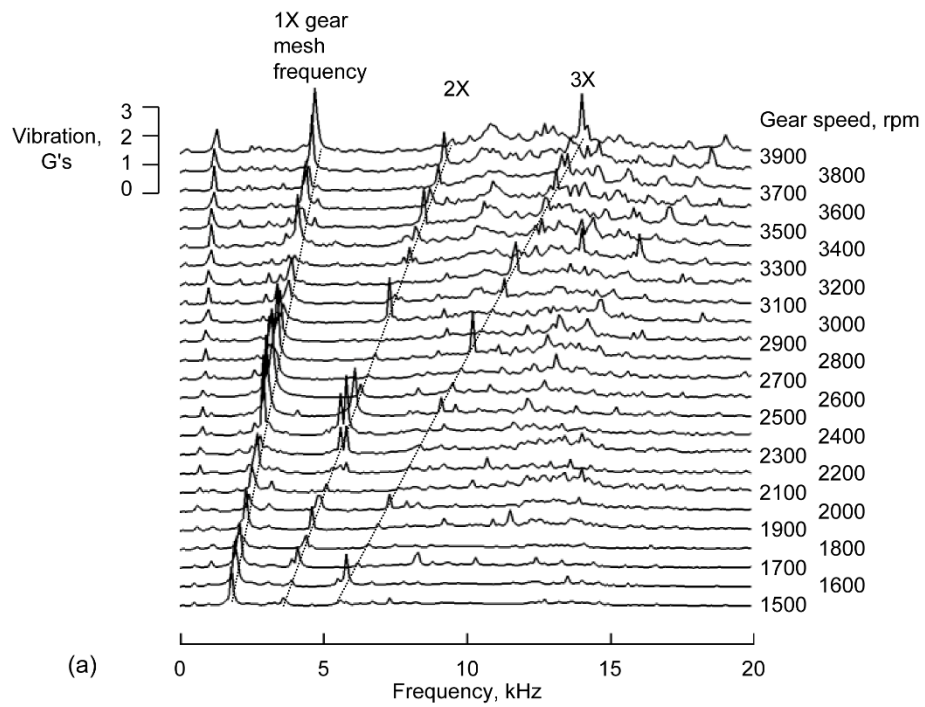


Figure 9.—Speed sweep test results for helical test gear set. (a) Left (test) side accelerometer. (b) Right (slave) side accelerometer.

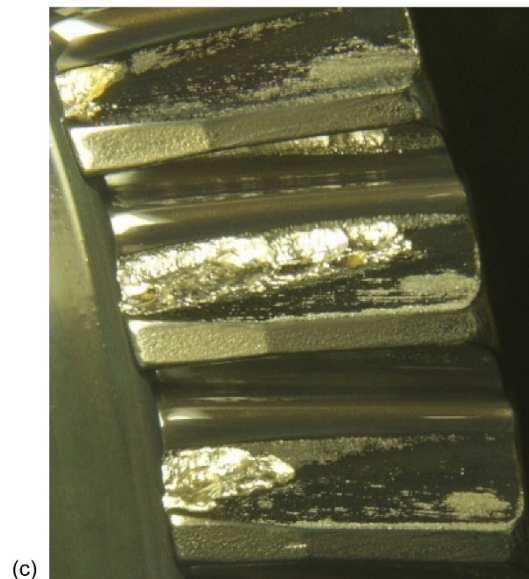
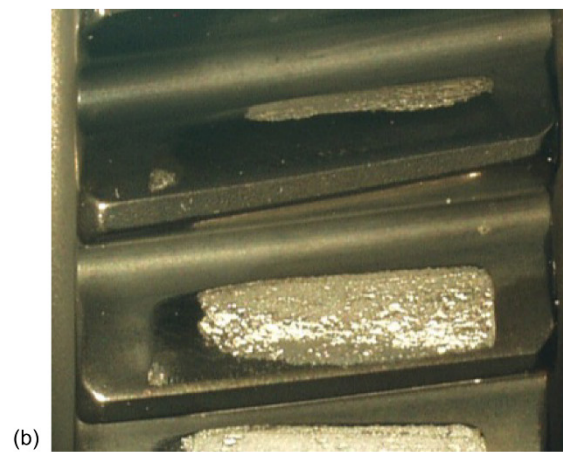
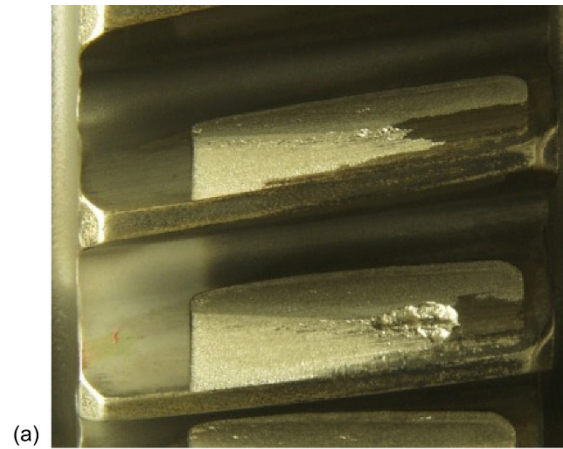


Figure 10.—Typical contact fatigue failures of helical test gear sets. (a) Pinion failure, contact fatigue, macropitting, spall. (b) Pinion failure, contact fatigue, macropitting, progressive. (c) Face gear failure, contact fatigue, macropitting, spall.



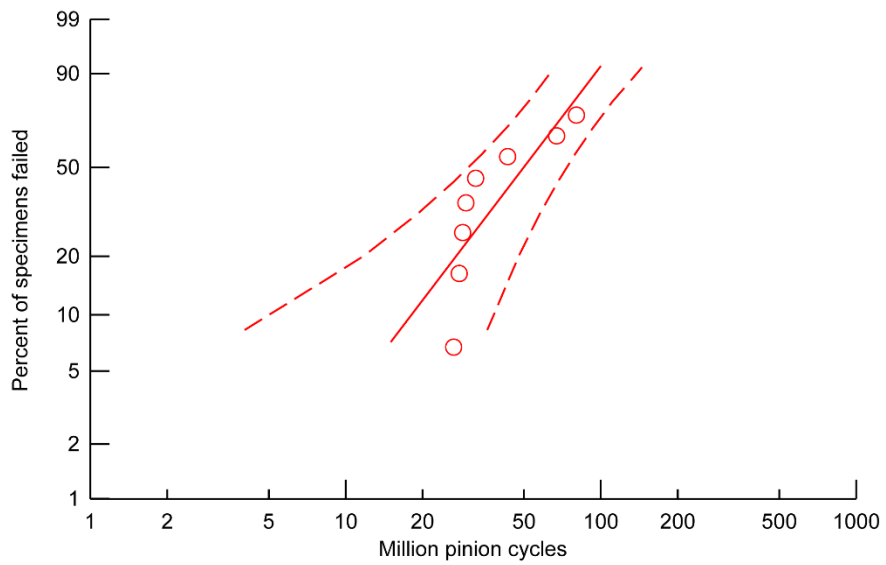
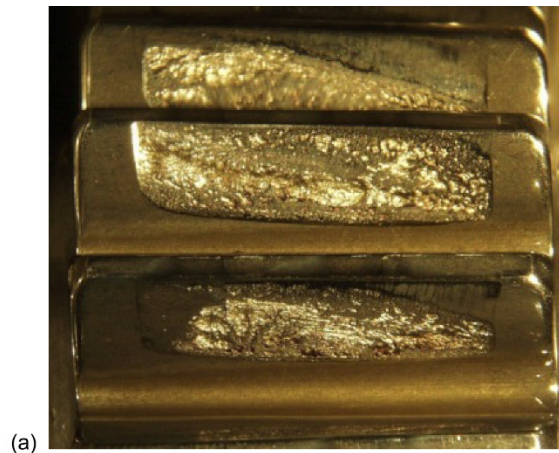


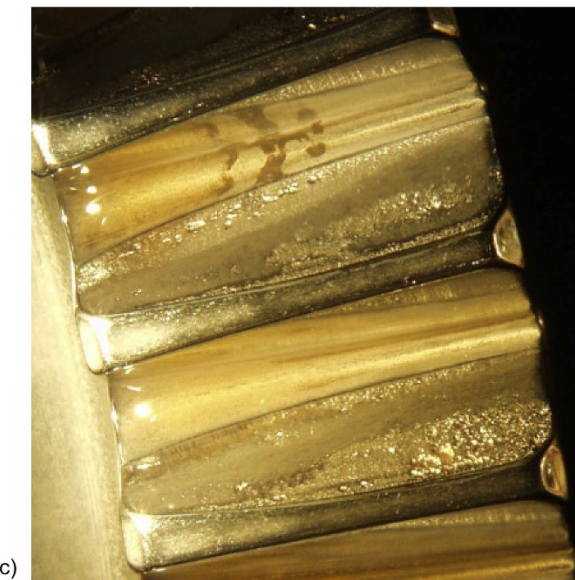
Figure 11.—Weibull plot with 90% confidence bands for contact fatigue failures of helical test gear sets.



(a)



(b)



(c)

Figure 12.—Typical contact fatigue failures of ISF test gear sets. (a) Pinion failure, contact fatigue, macropitting, spall. (b) Pinion failure, contact fatigue, macropitting, progressive. (c) Face gear failure, contact fatigue, macropitting, progressive.

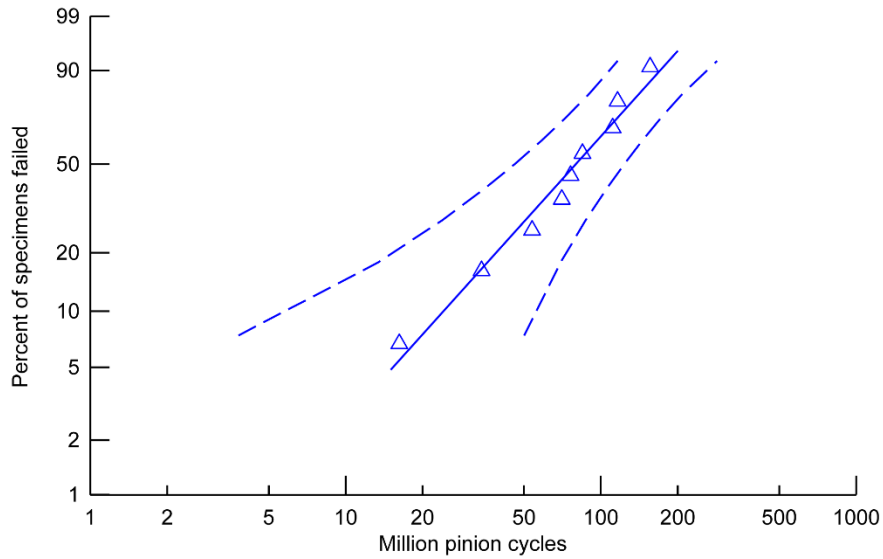


Figure 13.—Weibull plot with 90% confidence bands for contact fatigue failures of ISF test gear sets.

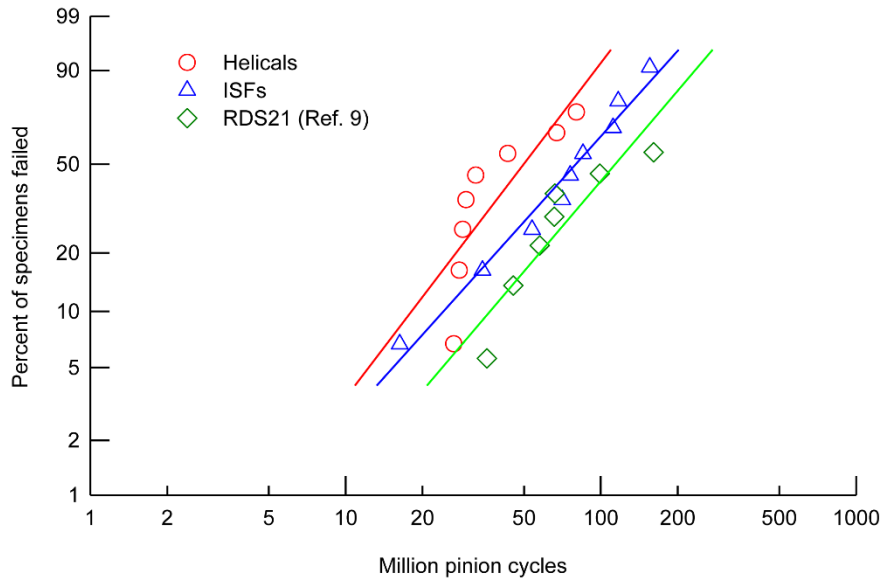


Figure 14.—Weibull plot with 90% confidence bands for contact fatigue failures, comparison of helical test gear sets, ISF test gear sets, and RDS21 test gear sets.





